arXiv:astro-ph/0701274v1 9 Jan 2007

Dependence of Heliospheric Lyα Absorption on the Interstellar Magnetic Field

Brian E. Wood[1], Vladislav V. Izmodenov[2,3], Jeffrey L. Linsky[1], Dmitry Alexashov[3]

ABSTRACT

We use newly developed 3D kinetic MHD models of the heliosphere to predict heliospheric H I Lyα absorption for various lines of sight. These predictions are compared with actual Lyα spectra from the *Hubble Space Telescope*, many of which have yielded previous detections of heliospheric absorption. We find that the absorption predicted by the models is weakly affected by both the magnitude and orientation of the assumed ISM magnetic field. Models with $B = 1.25 - 2.5$ μG and an angle of $\alpha = 15 - 45^\circ$ with respect to the upwind direction of the ISM flow generally provide the best fits to the data, but the sensitivity of the Lyα absorption to many model input parameters makes it difficult to fully characterize the region of parameter space allowed by the data. We also use the models to assess the degree to which heliospheric asymmetries induced by the ISM field should be apparent in Lyα absorption. An ISM field that is skewed with respect to the ISM flow vector results in substantial azimuthal asymmetries in both the hydrogen wall and heliosheath, but only the heliosheath asymmetries yield potentially detectable asymmetries in Lyα absorption; and then only in downwind directions, where comparison with the data is complicated by few actual absorption detections and an insufficient model grid extent.

Subject headings: MHD — solar wind — interplanetary medium — ultraviolet: stars

[1]JILA, University of Colorado, 440 UCB, Boulder, CO 80309-0440; woodb@origins.colorado.edu, jlinsky@jila.colorado.edu.

[2]Lomonosov Moscow State University, Dept. of Aeromechanics and Gas Dynamics, Moscow 119899, Russia; izmod@ipmnet.ru.

[3]Institute for Problems in Mechanics RAS, Prospekt Vernadskogo 101-1, Moscow 117526, Russia; and Space Research Institute (IKI) RAS

1. INTRODUCTION

The interaction region between the solar wind and ambient ISM has been the subject of hydrodynamic modeling efforts (Parker 1961, 1963) since around the time of the first *in situ* observations of the solar wind by *Mariner 2* (Neugebauer & Snyder 1962) and by *Luna 2* (Gringauz et al. 1960). As shown in Figure 1, this interaction results in a large scale structure for the heliosphere that consists of three boundaries: the termination shock (TS), where the solar wind is shocked to subsonic speeds; the bow shock (BS), where the ISM flow is shocked to subsonic speeds; and in between the two the heliopause (HP), which separates the plasma flows of the fully ionized solar wind and partially ionized ISM. Reviews of the history of heliospheric modeling include Holzer (1989), Baranov (1990), Zank (1999), and Baranov & Izmodenov (2006).

Voyager 1 recently encountered the TS at a distance of 94 AU from the Sun in roughly the upwind direction relative to the ISM flow (Stone et al. 2005). However, the locations of the more distant HP and BS remain observationally uncertain. In general, there are very few observational constraints for the properties of the heliosphere beyond the TS. One of the few exceptions is heliospheric Lyα absorption, which is observable in *Hubble Space Telescope* (HST) spectra of nearby stars.

Unlike the ionized component of the ISM, the neutrals in the ISM can penetrate into all regions of the heliosphere. Charge exchange processes involving these neutrals create populations of hot H I that permeate the heliosphere, and it is these neutrals that produce absorption signatures in stellar Lyα lines observed by HST. For most lines of sight, the absorption is dominated by H I in the so-called "hydrogen wall" region in between the HP and BS (Baranov et al. 1991; Wood et al. 2005b), but in downwind directions absorption from heliosheath neutrals, created by charge exchange between the TS and HP, can be paramount (Izmodenov et al. 1999; Wood et al. 2007). The heliospheric absorption is only detectable when the ISM absorption for the observed line of sight is not too broad to obscure the absorption. In upwind directions the interstellar H I column density (in cm^{-2}) must be $\log N(\mathrm{H\ I}) < 18.2$ to detect heliospheric absorption, but in downwind directions one must have $\log N(\mathrm{H\ I}) < 17.8$ (Wood et al. 2005a). Astrospheric absorption from the wind-ISM interaction region surrounding the observed star can also sometimes be detected.

Starting with Gayley et al. (1997), there have been many attempts to use the Lyα absorption observations to test heliospheric models. The hydrodynamic models are generally quite successful in reproducing the observed amount of absorption, especially in upwind directions where the hydrogen wall accounts for most of it (Gayley et al. 1997; Izmodenov et al. 1999, 2002; Wood et al. 2000). The Lyα absorption therefore represents a convincing detection of the hydrogen wall, and a validation of the models that predicted it even before it was

detected by HST.

However, the exact amount of absorption predicted by the models is dependent on the parameters that are assumed for the Local Interstellar Cloud (LIC) in which the Sun resides (Lallement & Bertin 1992). Some aspects of the ambient ISM are known very well, such as the LIC flow speed and direction (e.g., Witte 2004; Möbius et al. 2004), but others are not known as precisely. Thus, there has been hope that the Lyα absorption can help constrain certain properties of the ISM. Izmodenov et al. (2002), for example, experimented with numerous different models assuming different combinations of ISM proton and H I densities. The absorption predicted by the models does vary with the input parameters, but the absorption diagnostic seems to have only a modest sensitivity to most input parameters of interest, making it difficult to simply define a range of parameters that are consistent with the data. The dependence of the predicted absorption on the nature of the hydrodynamic code used in the modeling is also a problem (Wood et al. 2000; Izmodenov et al. 2002). The source of this difficulty lies in the complexity of H I velocity distributions within the heliosphere, which are non-Maxwellian (e.g., Izmodenov et al. 2001) and therefore can only be modeled with fully kinetic or complex multi-fluid codes.

All of the models that have been compared with the data in the past have been 2-dimensional, axisymmetric models. Recently, 3-dimensional MHD models have become available that are capable of considering the effects of the ISM magnetic field on heliospheric structure, while still maintaining a sufficiently sophisticated treatment of the neutrals to properly consider them and the plasma in a self-consistent manner (Izmodenov et al. 2005; Izmodenov & Alexashov 2006; Pogorelov & Zank 2006). Figure 1 presents results of calculations made with a 3D kinetic MHD model of the heliosphere by Izmodenov et al. (2005). It shows that the inclusion of even a modest ISM field can indeed affect the shape of the global heliosphere. We will determine here whether this also has significant effects on the Lyα absorption. The nature of the magnetic field in the ISM immediately outside the heliosphere is poorly known, so we will also assess the sensitivity of the Lyα absorption to changes in the assumed ISM field strength and orientation. In doing so, we consider many more HST-observed lines of sight than have been used in prior data-model comparisons.

2. THE CHOSEN SAMPLE OF HST Lyα OBSERVATIONS

The amount of heliospheric Lyα absorption depends greatly on the direction of the observed line of sight. The greatest spatial dependence is on the poloidal angle θ between the line of sight and the upwind direction of the ISM flow. Clearly it is advantageous to consider many different lines of sight with a wide variety of θ's in comparing the heliospheric

absorption predicted by models with the data. Considering a variety of directions is even more important when testing 3D MHD models, which can yield heliospheric structures that are not axisymmetric and therefore will have absorption predictions that are dependent on the azimuthal angle as well as being dependent on θ (see Fig. 1). Past data-model comparisons considered no more than six HST-observed lines of sight, which individually have either provided real detections of heliospheric absorption or merely upper limits (Wood et al. 2000; Izmodenov et al. 2002). This is a rather small number of lines of sight even for testing axisymmetric models, let alone the 3D ones. However, the number of heliospheric absorption detections has recently increased significantly (Wood et al. 2005b, 2007), so it is well worthwhile to reassess the sample of available HST data to select a larger sample of spectra to test the 3D kinetic MHD models.

Wood et al. (2005b) provide a complete list of HST-observed Lyα spectra that are appropriate for our purposes, all of which have been analyzed to measure ISM H I column densities, to search for evidence of heliospheric/astrospheric absorption, and to measure stellar Lyα fluxes corrected for the contaminating ISM absorption. Figure 2 is a sky map in ecliptic coordinates of lines of sight with a stellar Lyα line observed by HST. All these spectra have sufficient spectral resolution to permit a reasonably precise search for heliospheric absorption. The boxes indicate the 11 lines of sight that actually yield detections of heliospheric absorption. All the other lines of sight yield nondetections.

Many of the detections are clustered around the upwind direction of the ISM flow. The advantageous nature of upwind lines of sight for detecting heliospheric absorption is consistent with model predictions, which suggest that the deceleration of H I in the hydrogen wall relative to the ISM flow should be largest in these directions. This results in a greater separation of the heliospheric absorption from that of the ISM, thereby making it easier to detect heliospheric absorption in upwind lines of sight (Wood et al. 2005b).

There is also a cluster of three detections very close to the downwind direction. Initial analysis of these Lyα spectra did *not* yield detections (Wood et al. 2005b). However, we have found that the stellar Lyα profiles reconstructed for $\theta > 160^\circ$ lines of sight are systematically blueshifted from the stellar rest frames, indicating the presence of very broad, shallow absorption on the red side of the Lyα profiles (Wood et al. 2007). This is the exactly the sort of absorption signature one expects from heliosheath neutrals (as opposed to hydrogen wall neutrals). Since very downwind lines of sight looking down the tail of the heliosphere will have very long path lengths through the heliosheath, it is in the most downwind lines of sight where one might expect to see this broad absorption. Thus, we now consider these three lines of sight to have detections of heliospheric absorption, though the nature of these detections is rather different from the others.

Our goal is to select a sample of HST-observed lines of sight from Figure 2 to use for comparing observed and predicted heliospheric Lyα absorption. Obviously we start by choosing the 11 detections, which actually provide quantitative measurements of the absorption. We add to these detections nine nondetections (diamonds in Fig. 2) that at least provide upper limits for the amount of absorption that might be present in those directions. These nondetections are chosen to sample parts of the sky not covered by the detections. Another major selection criterion is ISM H I column density. Lines of sight with low ISM column densities are preferable since they provide more restrictive upper limits on heliospheric absorption. Data quality (i.e., resolution, signal-to-noise) also plays a role in choosing which nondetections to consider.

Numbered symbols in Figure 2 indicate the final sample of 20 lines of sight to be used in our data-model comparisons. The stellar identifications of these lines of sight are indicated in Figures 3 and 4, along with the Lyα spectra, which are displayed in order of increasing θ. We focus only on the red side of the Lyα absorption profile, where the heliospheric absorption resides. The fluxes are normalized to the intrinsic stellar Lyα profile reconstructed in the original analysis of the data. We refer the reader to Wood et al. (2005b) and references therein to see the full Lyα spectra and descriptions of their analysis. The dotted green lines in the figure show only the ISM absorption based on these analyses. For the heliospheric absorption detections, there is excess absorption observed beyond that from the ISM. Successful heliospheric models should predict the right amount of excess absorption to fit the data for these lines of sight. For the nondetections, the ISM absorption fits the data reasonably well. In these cases, successful heliospheric models should predict essentially no significant absorption beyond that from the ISM.

The three $\theta > 160^\circ$ detections (#18–#20 in Figs. 2–4) are special cases, as mentioned above. The original reconstructed stellar Lyα profiles suggest no heliospheric absorption, but the blueshifts of these profiles away from their stellar rest frames implies that these profiles are inaccurate. We can infer the amount of heliospheric absorption in these directions by constructing a stellar profile forced to be centered on the stellar radial velocity and then seeing how much of the red wing of that profile must be absorbed to yield the original profile. The shaded regions in Figure 3 for these three downwind lines of sight indicate this excess absorption, where the uncertainties are estimated by allowing the stellar radial velocity to be ± 3 km s^{-1} from its measured value. This excess absorption cannot be extended to lower velocities closer to the center of the Lyα line because near line center stellar Lyα profiles cannot be assumed to be symmetric and centered on the stellar rest frame. Stellar Lyα profiles often have self-reversals near line center, which are often asymmetric. For details about all of this, see Wood et al. (2007). The important thing to note here is that for these three very downwind lines of sight, the absorption predicted by the models should *not* fit

the data but should instead fall within the shaded regions.

Finally, the requirement that the intrinsic stellar Lyα profile be within ± 3 km s^{-1} of the stellar rest frame allows us to compute upper limits for the amount of broad heliosheath absorption that can be present for lines of sight without detected heliospheric absorption. Thick dashed lines in Figure 3 show these upper absorption limits, but only for downwind lines of sight ($\theta > 110°$) where the broad heliosheath absorption is potentially prominent. Absorption predictions from the models must lie above these limits to be consistent with the data. The dashed lines cannot be extended to low velocities close to line center for the same reason that the shaded regions of the $\theta > 160°$ lines of sight are limited to the wings of the line (see above).

3. THE INTERSTELLAR MAGNETIC FIELD'S EFFECTS ON Lyα ABSORPTION

Figures 3 and 4 compare the HST Lyα data with the heliospheric absorption predicted by 3D kinetic MHD models of the heliospheric interface (Izmodenov et al. 2005; Izmodenov & Alexashov 2006), assuming various directions and magnitudes for the ISM field. The models used here are of the type initially developed by Baranov & Malama (1993, 1995), with a fully kinetic treatment of neutral hydrogen within the heliosphere to provide the most precise computations of the velocity distribution functions of the neutrals. Izmodenov et al. (2005) expanded the 2D axisymmetric Baranov & Malama code to a fully 3D geometry, and also added the capability of including an interstellar magnetic field in the model. The code separates all heliospheric H atoms into several populations: 1. original interstellar atoms and other atoms originating outside of the bow shock, 2. secondary interstellar atoms originating between the bow shock and heliopause, 3. atoms originating between the heliopause and termination shock, and 4. atoms originating in the supersonic solar wind. We calculate number densities, temperatures, and bulk velocities for these populations along the lines of sight toward the observed stars by taking moments of the velocity distributions. The heliospheric absorption for each line of sight is computed from these traces of density, temperature, and flow velocity. With this methodology, we are making the approximation that the velocity distribution functions of the individual populations are locally Maxwellian.

3.1. Previous Constraints on the Local ISM Field

The nature of the interstellar magnetic field surrounding the Sun is poorly known, though some observational constraints exist. The global Galactic field has a magnitude of 1.6 ± 0.2 μG and is directed towards a Galactic longitude of $l = 96 \pm 4°$, but there is substantial local variability (Rand & Kulkarni 1989), meaning that the actual local field could be significantly higher or lower and could be in a completely different direction.

A $\sim 4°$ discrepancy exists between the flow vectors of interstellar He and H within the solar system, and the most promising explanation for this is that the LIC's magnetic field is skewed with respect to the ISM flow seen by the Sun, which can deflect the flow of interstellar hydrogen atoms in the heliosphere (Lallement et al. 2005). Helium atoms are not affected in this manner, since their charge exchange cross sections are much lower than hydrogen and they are therefore effectively blind to the presence of the heliosphere. If correct, this interpretation identifies a plane in which the ISM field must lie, which happens to be inconsistent with the orientation of the global Galactic field. Opher et al. (2006) have argued that an ISM field that is $\alpha = 30° - 60°$ from the apparent flow direction can potentially explain *Voyager 1* and *2* observations of energetic particles flowing inwards from the TS. The satellites have both seen these particles, but flowing in opposite directions. Opher et al. (2006) demonstrate that asymmetries in the heliospheric structure induced by a skewed ISM magnetic field can potentially cause this effect, thanks in part to the satellites' positions on opposite sides of the ecliptic plane.

A magnetic field much stronger than the global Galactic field has been proposed to explain an apparent pressure imbalance between the hot, ionized plasma that dominates the Local Bubble and the warm, partially neutral clouds that lie within it. The Local Bubble, the cavity in which the Sun resides (Lallement et al. 2003), is believed to account for much of the soft X-ray background radiation (see also Smith et al. 2006). These X-rays seem to suggest thermal pressures of $P/k \sim 15,000$ cm^{-3} K (Snowden et al. 1998). In contrast, the LIC and other warm clouds within the Local Bubble appear to have much lower pressures of $P/k \sim 2280$ cm^{-3} K (Jenkins 2002; Redfield & Linsky 2004). Such a large pressure imbalance within the local ISM seems unlikely.

One way out of this dilemma is to propose that the LIC is supported by a strong magnetic field of order 7 μG (Cox & Helenius 2003; Florinski et al. 2004). This would seem to be disallowed by heliospheric models, which imply that such large magnetic pressures would force the termination shock well inside the 94 AU distance measured by *Voyager 1* (Gloeckler et al. 1997; Stone et al. 2005). The only way to avoid this problem is for the field to be nearly parallel to the ISM flow. However, this would contradict the evidence mentioned above that the LIC field is *not* parallel to to the LIC flow (i.e., the discrepant H

and He flow vectors within the solar system, and the opposite flow directions of termination shock particles observed by *Voyager 1* and *2*). Thus, large fields are still difficult to reconcile with heliospheric observations and models. An alternative solution to the Local Bubble pressure problem is that the pressures normally estimated from the soft X-ray emission are too high for various reasons: contamination from heliospheric foreground emission (Cravens 2000; Lallement 2004a; Koutroumpa et al. 2006), contamination from X-ray emission from the walls of the Local Bubble (Lallement 2004b), and improper assumption of collisional ionization equilibrium (Breitschwerdt 2001).

3.2. Absorption Constraints on the ISM Field

Most of our models are computed assuming a modest magnetic field of $B = 2.5$ μG, which can compress the TS somewhat depending on the field orientation, but not enough to be inconsistent with the *Voyager 1* encounter distance of 94 AU (see Fig. 1). We assume that the magnetic field is oriented within the plane suggested by Lallement et al. (2005). Figure 3 shows the absorption predicted by models with different field orientations within this plane, for angles ranging from parallel to the ISM flow ($\alpha = 0°$) to perpendicular to the ISM flow ($\alpha = 90°$). Table 1 lists the ecliptic and Galactic coordinates that correspond to these field directions. Figure 4 shows the absorption predictions for three models with $\alpha = 45°$, but with different field strengths of 0, 1.25, and 2.5 μG. The ISM hydrogen and proton densities assumed in these models are $n_\infty(H\ I) = 0.18$ cm^{-3} and $n_\infty(H^+) = 0.06$ cm^{-3}, the ISM flow speed is $V_\infty = 26.4$ km s^{-1}, and the temperature is $T_\infty = 6400$ K (Izmodenov et al. 2005).

Figure 3 shows that in upwind directions, where most of the heliospheric detections lie, the absorption decreases with increasing α. To better illustrate this behavior, Figure 5 plots the absorbed Lyα flux predicted by the Figure 3 models versus α. No one model clearly fits the data better than all the others, presumably due to the absorption dependence on α being only a modest one. This also may be indicative of the systematic uncertainties in the estimation of the ISM absorption. The 61 Vir line of sight seems particularly discrepant. This is probably due to difficulties in removing geocoronal emission blended with the red side of the Lyα absorption line (see Fig. 1 in Wood et al. 2005b), so this line of sight should be regarded with caution.

The $\alpha = 60°$ and $\alpha = 90°$ models underestimate the absorption in all upwind directions (see Figs. 3 and 5), so perhaps these models should be considered inconsistent with the data. If one ignores the problematic 61 Vir line of sight, the $\alpha = 0°$ model is a worse fit to the data than the $\alpha = 15° - 45°$ for all but the 36 Oph line of sight. Considering the evidence described above that the ISM field is skewed from the flow direction, $\alpha = 0°$ seems unlikely

anyway. Thus, we consider $\alpha = 15° - 45°$ to represent the most likely field orientations for the local ISM, which overlaps the $\alpha = 30° - 60°$ range quoted by Opher et al. (2006).

These conclusions are based on $B = 2.5$ μG models, but Figure 4 shows that assuming $B = 1.25$ μG does not change the absorption very much. Thus, at least for these low-to-moderate field strengths our conclusions concerning α are relatively sound. However, Figure 4 shows that decreasing the field all the way to zero does change the absorption, with the absorption being somewhat higher in upwind directions. The greater amount of absorption upwind is somewhat surprising considering that the hydrogen wall is narrower for $B = 0$ (see Fig. 1). However, the inclusion of even a modest ISM field weakens the bow shock and lowers the H I density in the hydrogen wall, more than offsetting the broader width of the wall.

It should be stated that definitive conclusions are difficult to make at this point since the Lyα absorption is at least somewhat sensitive to other input parameters, such as the assumed ISM densities and temperature that also have observational uncertainties (Izmodenov et al. 2002), though not nearly as large as those involving the magnetic field. A time-consuming thorough exploration of parameter space would be necessary to fully characterize the constraints on ISM properties provided by the Lyα data.

We have focused so far on comparing the models with data in upwind directions, where absorption from the hydrogen wall is dominant. Any conclusions drawn from downwind directions, where heliosheath absorption is more prominent, will be far more tentative. The primary reason for this is that the grid used for our current models only extends 500 AU from the Sun, which is not nearly far enough to capture all of the heliosheath absorption for $\theta \gtrsim 120°$. Thus, the absorption predictions shown in Figures 3 and 4 for these directions will underestimate the amount of absorption that the models would really predict if the grid were extended further downwind.

Many of the models seem to predict too much absorption downwind even with the limited grid extent, particularly in the velocity range of $80 - 120$ km s^{-1}. But there is another potential difficulty with downwind absorption that concerns the treatment of the plasma in the models. Although a fully kinetic treatment is applied to the neutrals, the plasma is assumed to be a single Maxwellian fluid throughout the heliosphere. However, this is clearly a poor approximation, since pickup ions, for example, have non-Maxwellian velocity distributions and are not thermalized with the solar wind inside the termination shock (e.g., Gloeckler & Geiss 2004). Malama et al. (2006) have replaced the simple single-fluid plasma treatment in the 2D Baranov & Malama code with a complex multi-component representation of the plasma. This more sophisticated plasma treatment does not result in significantly different hydrogen wall absorption in upwind directions, but we have found that is *does* result

in a significant reduction in heliosheath absorption which can potentially alleviate the problems these models have in predicting too much downwind absorption (Wood et al. 2007). The most meaningful comparison with the data in downwind directions would therefore require that our 3D models also utilize such a multi-component plasma treatment, as well as having grids that extend far enough downwind to capture all the heliosheath absorption. We leave such computationally intensive modeling for a future paper.

We note that asymmetries in the heliospheric structure induced by the ISM field are evident in the downwind absorption predicted by the models. For example, there is significant model dependence in the absorption towards DK UMa ($\theta = 112°$), but no significant model dependence towards τ Cet ($\theta = 123°$). Since θ is similar for these stars but their azimuthal angles quite different (see Fig. 2), this difference in behavior must be due to azimuthal variability, which can only be due to magnetic field induced asymmetries (see §3.3).

Finally, we note that Pogorelov & Zank (2006) have also developed 3D MHD heliospheric models that treat neutrals in a self-consistent manner with the plasma. This code uses a less sophisticated 2-fluid treatment for the neutral H velocity distributions, but it includes the effects of the interplanetary magnetic field on heliospheric structure as well as the ISM field. Absorption has been computed for a limited number of these models, yielding results qualitatively similar to those reported here, with absorption decreasing with both α and the magnetic field strength (Wood et al. 2006). Like Izmodenov et al. (2005), Pogorelov & Zank (2006) demonstrate that the 3D MHD models can potentially reproduce the shift between the H and He flows observed within the solar system (Lallement et al. 2005), though they emphasize that the magnitude of the shift depends not only on the strength and orientation of the magnetic field, but also on the ISM neutral hydrogen density.

3.3. Quantifying Expected Absorption Asymmetries

Figure 1 illustrates that even a modest ISM field can result in a heliospheric structure that is significantly asymmetric, consistent with other models that also predict asymmetries of this sort (Ratkiewicz et al. 1998; Pogorelov & Zank 2006). In the bottom half of Figure 1, the heliosheath (between the TS and HP) is narrower than in the upper half, but the hydrogen wall (between the HP and BS) is wider. One might imagine that this would result in corresponding Lyα absorption asymmetries. In other words, the Lyα absorption should be azimuthally dependent as well as θ dependent.

Some evidence that the models do indeed predict azimuthally dependent absorption in downwind directions is mentioned in §3.2. However, in order to properly quantify the

degree of absorption asymmetry expected based on the models, it is necessary to compare absorption predictions for lines of sight with identical θ values but different azimuthal angles (ϕ). This cannot be easily done with the set of observed directions in Figures 3–4, which are scattered randomly about the sky.

Thus, in Figure 6 we show the heliospheric Lyα absorption predicted by the $B = 2.5$ μG, $\alpha = 45°$ model for various ϕ angles, with θ fixed in the five panels of the figure. The azimuthal angle is defined such that $\phi = 0°$ and $\phi = 180°$ are in the plane of the ISM magnetic field. This is the plane in which the heliospheric structure is portrayed in Figure 1. The $\phi = 0°$ direction would be associated with the upper half of Figure 1, and $\phi = 180°$ would be associated with the lower half.

In general, the hydrogen wall will be responsible for the steep, saturated absorption edges of the absorption profiles in Figure 6, which are particularly prominent in upwind directions (e.g., located at 20–30 km s^{-1} in the $\theta = 30°$ panel), while the heliosheath is responsible for the broad, unsaturated absorption wings that extend to high velocities, which become more prominent in downwind directions. Very little ϕ dependence is apparent in upwind directions. This is a bit surprising given the hydrogen wall asymmetries apparent in Figure 1. However, it turns out that azimuthal density variations in the hydrogen wall offset the azimuthal width dependence. For example, although the hydrogen wall is narrower for $\phi = 0°$ (corresponding to the upper half of Fig. 1) than for $\phi = 180°$ (corresponding to the lower half of Fig. 1), this is offset by higher hydrogen wall densities in the $\phi = 0°$ direction, so integrated H I column densities are actually not very different.

Figure 6 shows that for $\theta = 60 - 90°$, the particularly narrow hydrogen wall at $\phi = 0°$ results in somewhat less hydrogen wall absorption than other directions, but the difference is so small it would be very difficult to detect in practice. In contrast, the heliosheath is thicker at $\phi = 0°$ and Figure 6 shows that this does in fact lead to the broad heliosheath absorption being significantly stronger in this direction than others, though it is only in downwind directions ($\theta > 90°$) where this azimuthal dependence becomes potentially detectable. As discussed in §3.2, actual comparisons with the data are currently problematic in these directions. The asymmetries seen for the $\theta = 90°$ and $\theta = 120°$ surely extend to $\theta = 150°$ as well, but Figure 6 does not show this due to the limited grid extent of the models. According to Figure 6, the heliosheath absorption is at a minimum in directions normal to the plane of the ISM field ($\phi = 90°$ and $\phi = 270°$), indicative of magnetic compression of the heliosphere in those directions, leading to shorter distances through the heliosheath for those lines of sight.

4. SUMMARY

We have compared H I Lyα absorption profiles predicted by 3D kinetic MHD models of the heliosphere with a large selection of Lyα lines observed by HST, including many lines of sight with detected heliospheric absorption. The primary purpose of this comparison is to assess the sensitivity of the predicted absorption to changes in the ISM magnetic field properties assumed in the model. Our results are as follows:

1. We find that the H I Lyα absorption has a modest sensitivity to both the strength and orientation of the ISM magnetic field. Focusing on upwind directions where most of the HST detections of heliospheric absorption reside, the models presented here with $B = 1.25 - 2.5$ μG and $\alpha = 15 - 45^\circ$ appear to provide the best fits to the data, consistent with constraints from other sources (Gloeckler et al. 1997; Izmodenov et al. 2005; Lallement et al. 2005; Opher et al. 2006).

2. However, since the Lyα absorption is sensitive to other model input parameters, such as the ISM H I density, which have not been varied here, the region of parameter space that yields acceptable fits to the data will be complex. It will be very difficult, perhaps impossible, for the Lyα absorption by itself to yield a unique set of model input parameters that fit the data. Nevertheless, the dependence of the absorption on many ISM parameters means that the absorption does provide one constraint on heliospheric models that is worthy of consideration in assessing how precisely the models reproduce reality.

3. The models show that an ISM field that is skewed with respect to the ISM flow vector results in substantial azimuthal asymmetries in the heliospheric hydrogen wall. Surprisingly, these asymmetries do not result in significant asymmetries in Lyα absorption from the hydrogen wall, since densities within the wall vary in such a way as to cancel out the effects of the spatial asymmetries on hydrogen wall column densities.

4. The models also show that a skewed ISM field results in significant azimuthal asymmetries in the heliosheath, and unlike the hydrogen wall these asymmetries *do* yield significant azimuthal absorption dependence, at least in downwind directions where the heliosheath absorption is prominent. These directions are clearly the best places to look for azimuthal dependences in Lyα absorption, but there are problems with doing this in practice. One is simply that we have few downwind detections of heliospheric Lyα absorption. Another is that the heliosheath absorption that dominates in downwind directions should ideally be modeled using a complex multi-fluid plasma treatment. And finally, the model grid must be extended a much longer distance downwind than

present models to capture all the heliosheath absorption in these directions. We hope to perform such computationally intensive modeling in the future.

This work was supported by NASA grant NNG05GD69G to the University of Colorado. V. I. was also supported by RFBR grant 04-02-16559, the "Dynastia" Foundation, and the "Foundation in Support of Russian Science".

REFERENCES

Baranov, V. B. 1990, Space Sci. Rev., 52, 89

Baranov, V. B., Lebedev, M. G., & Malama, Y. G. 1991, 375, 347

Baranov, V. B., & Malama, Y. G. 1993, J. Geophys. Res., 98, 15157

Baranov, V. B., & Malama, Y. G. 1995, J. Geophys. Res., 100, 14755

Baranov, V. B., & Izmodenov, V. V. 2006, Fluid Dynamics, 41, in press

Breitschwerdt, D. 2001, Ap&SS, 276, 163

Cox, D. P., & Helenius, L. 2003, ApJ, 583, 205

Cravens, T. E. 2000, ApJ, 532, L153

Florinski, V., Pogorelov, N. V., Zank, G. P., Wood, B. E., & Cox, D. P. 2004, ApJ, 604, 700

Gayley, K. G., Zank, G. P., Pauls, H. L., Frisch, P. C., & Welty, D. E. 1997, ApJ, 487, 259

Gloeckler, G., Fisk, L. A., & Geiss, J. 1997, Nature, 386, 374

Gloeckler, G., & Geiss, J. 2004, Adv. Space Res., 34, 53

Gringauz, K. I., Bezrukikh, V. V., Ozerov, V. D., Rybchinskii, R. E. 1960, Sov. Akad. Doklady, 131, 1301

Holzer, T. E. 1989, ARA&A, 27, 199

Izmodenov, V.V., Gruntman, M., Malama, Y.G., J. Geophys. Res. 106 , 10681

Izmodenov, V., Alexashov, D., & Myasnikov, A. 2005, A&A, 437, L35

Izmodenov, V. V., Lallement, R., & Malama, Y. G. 1999, A&A, 342, L13

Izmodenov, V. V., Wood, B. E., & Lallement, R. 2002, J. Geophys. Res., 107, 1308

Izmodenov, V. V., & Alexashov, D. B. 2006, in The Physics of the Inner Heliosheath: Voyager Observations, Theory, and Future Prospects, ed. J. Heerikhuisen, et al. (Melville, NY: AIP), 14

Jenkins, E. B. 2002, ApJ, 580, 938

Koutroumpa, D., Lallement, R., Kharchenko, V., Dalgarno, A., Pepino, R., Izmodenov, V., & Quémerais, E. 2006, A&A, 460, 289

Lallement, R. 2004a, A&A, 418, 143

Lallement, R. 2004b, A&A, 422, 391

Lallement, R., & Bertin, P. 1992, A&A, 266, 479

Lallement, R., Quémerais, E., Bertaux, J. L., Ferron, S., Koutroumpa, D., & Pellinen, R. 2005, Science, 307, 1447

Lallement, R., Welsh, B. Y., Vergely, J. L., Crifo, F., & Sfeir, D. M., 2003, A&A, 411, 447

Malama, Y. G., Izmodenov, V. V., & Chalov, S. V. 2006, A&A, 445, 693

Möbius, E., et al. 2004, A&A, 426, 897

Neugebauer, M., & Snyder, C. 1962, Science, 138, 1095

Opher, M., Stone, E. C., & Liewer, P. C. 2006, ApJ, 640, L71

Parker, E. N. 1961, ApJ, 134, 20

Parker, E. N. 1963, Interplanetary Dynamical Processes (New York: Interscience)

Pogorelov, N. P., & Zank, G. P. 2006, ApJ, 636, L161

Rand, R. J., & Kulkarni, S. R. 1989, ApJ, 343, 760

Ratkiewicz, R., Barnes, A., Molvik, G. A., Spreiter, J. R., Stahara, S. S., Vinokur, M., & Venkateswaran, S. 1998, A&A, 335, 363

Redfield, S., & Linsky, J. L. 2004, ApJ, 613, 1004

Smith, R. K., et al. 2006, PASJ, in press

Snowden, S. L., Egger, R., Finkbeiner, D. P., Freyberg, M. J., & Plucinsky, P. P. 1998, ApJ, 493, 715

Stone, E. C., Cummings, A. C., McDonald, F. B., Heikkila, B. C., Lal, N., and Webber, W. R. 2005, Science, 309, 2017

Witte M. 2004, A&A, 426, 835

Wood, B. E., Izmodenov, V. V., Linsky, J. L., & Malama, Y. G. 2007, ApJ, in press

Wood, B. E., Izmodenov, V. V., & Pogorelov, N. V. 2006, in The Physics of the Inner Heliosheath: Voyager Observations, Theory, and Future Prospects, ed. J. Heerikhuisen, et al. (Melville, NY: AIP), 335

Wood, B. E., Müller, H. -R., & Zank, G. P. 2000, ApJ, 542, 493

Wood, B. E., Müller, H. -R., Zank, G. P., Linsky, J. L., & Redfield, S. 2005a, ApJ, 628, L143

Wood, B. E., Redfield, S., Linsky, J. L., Müller, H. -R., & Zank, G. P. 2005b, ApJS, 159, 118

Zank, G. P. 1999, Space Sci. Rev., 89, 413

This preprint was prepared with the AAS LaTeX macros v5.2.

Table 1. Model ISM Field Orientations

α (deg)	Ecliptic Coord.		Galactic Coord.	
	l_e (deg)	b_e (deg)	l (deg)	b (deg)
0	74.7	−5.2	183.3	−15.9
15	66.9	−18.1	191.9	−28.6
30	57.8	−30.6	202.7	−40.6
45	46.1	−42.4	218.2	−51.2
60	29.5	−52.4	241.0	−58.7
90	335.8	−59.6	298.2	−56.0

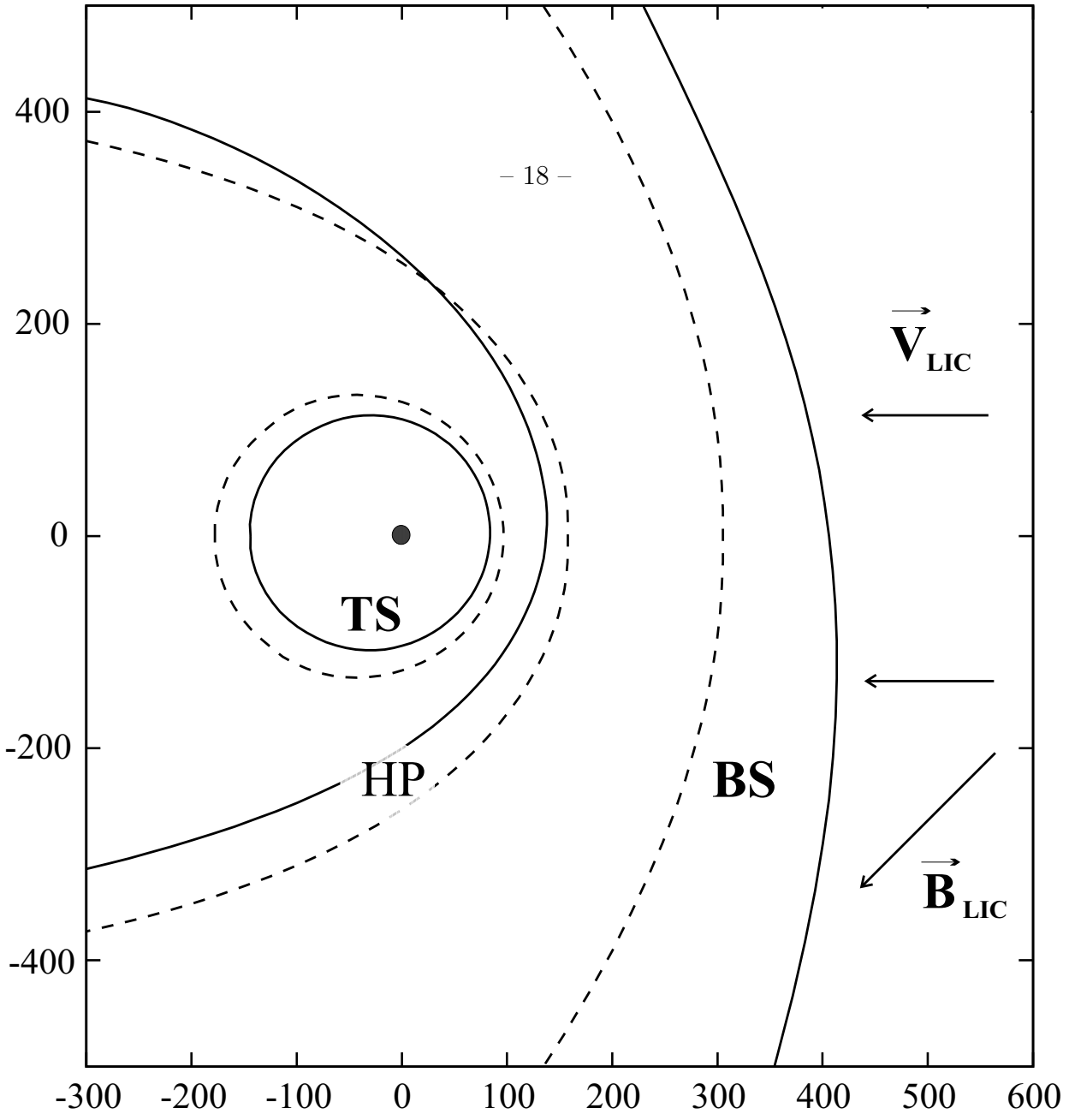

Fig. 1.— The locations of the termination shock (TS), heliopause (HP), and bow shock (BS) for a model including a $B = 2.5$ μG ISM field (solid lines), and a model with no ISM magnetic field (dashed lines). The directions of the LIC flow vector (V_{LIC}) and magnetic field (B_{LIC}) are indicated. The distance scale is in AU. The region between the HP and BS is sometimes called the "hydrogen wall" and the region between the TS and HP is the "heliosheath."

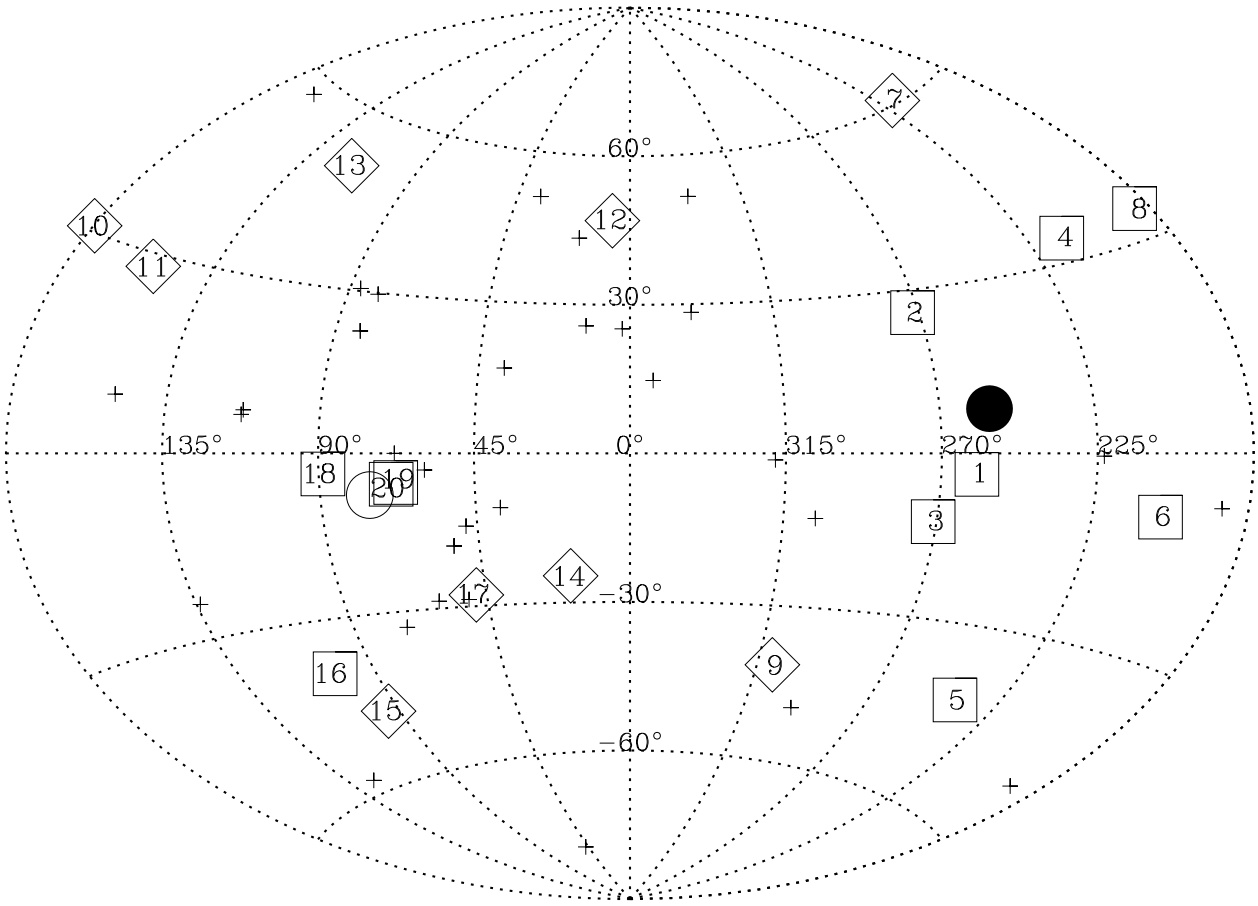

Fig. 2.— Sky map in ecliptic coordinates of all HST-observed lines of sight with useful Lyα spectra. The numbered symbols indicate spectra that we will compare with model predictions of Lyα absorption (see Figs. 3 and 4). Boxes indicate lines of sight with detected heliospheric absorption. The plus signs and diamonds are both lines of sight with nondetections of heliospheric absorption. The diamonds indicate lines of sight selected to provide upper limits for absorption in those directions. The filled and open circles indicate the upwind and downwind directions of the local ISM flow vector, respectively.

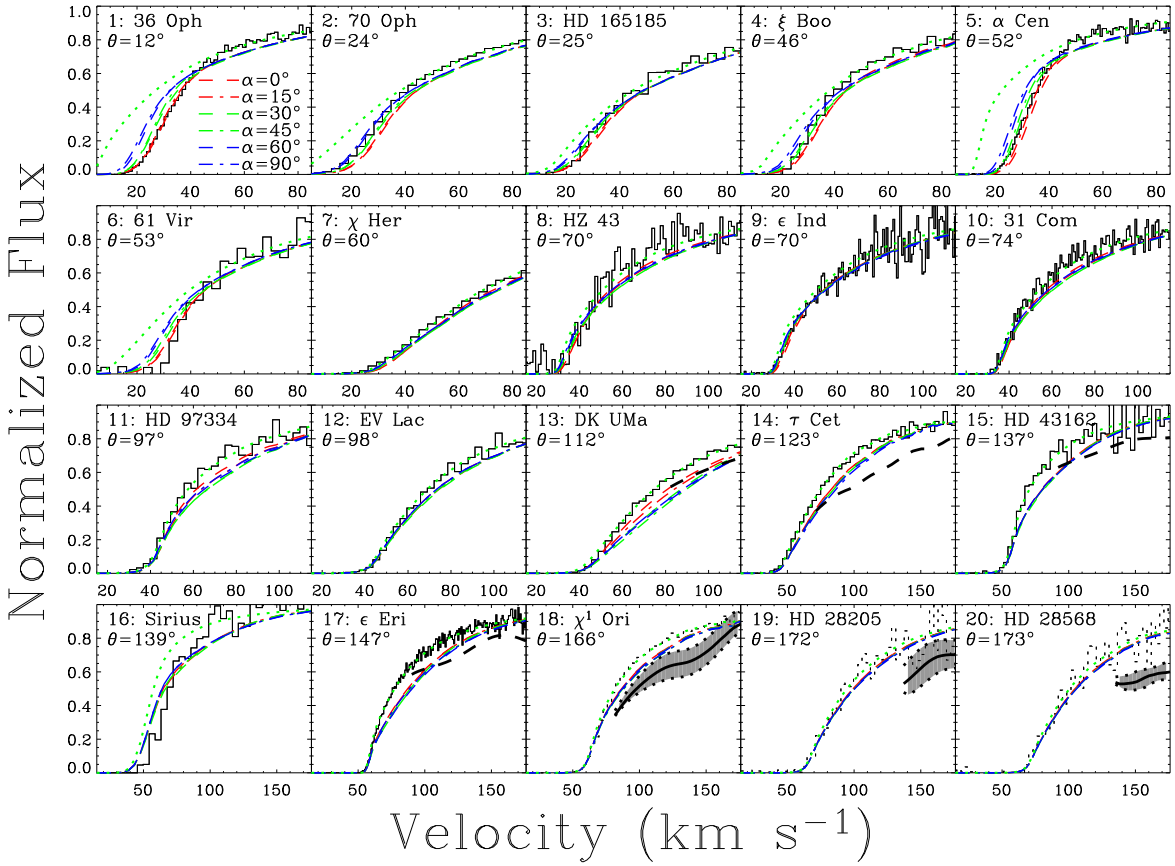

Fig. 3.— The red side of the H I Lyα absorption line (histogram) for the selected stars from Fig. 2, where the stars are placed in order of increasing angle from the upwind direction of the ISM flow (θ). In each panel, the dotted green line is the ISM absorption alone. Absorption predictions are shown for heliospheric models computed assuming six different ISM field orientations, as quantified by α, the angle between the field and the ISM flow direction (see the 36 Oph panel for line identifications). For many downwind lines of sight ($\theta > 110°$), dashed lines show upper limits to the amount of absorption that can be present — absorption predictions from the models must lie above these limits to be consistent with the data. For the three most downwind lines of sight, the shaded regions indicate the amount of absorption that the models *should* predict if the real stellar Lyα profile is centered on the stellar rest frame rather than blueshifted as suggested by the original recontructed profile. For these lines of sight, the absorption predicted by the models should not fit the data (which are dotted histograms in these cases) but should instead fall within the shaded regions (see §2).

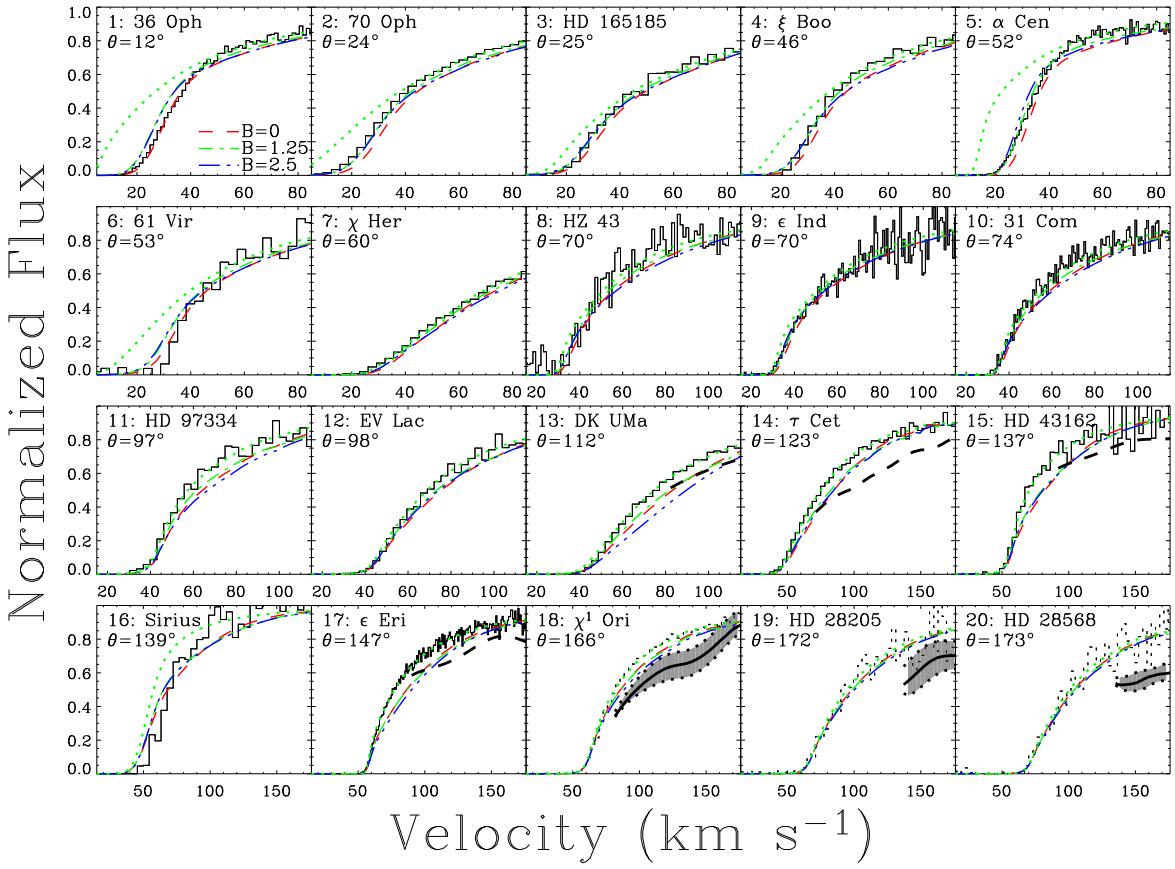

Fig. 4.— A figure analogous to Fig. 3, but in this case the absorption predictions are for three $\alpha = 45°$ models that assume different ISM magnetic field strengths (see the 36 Oph panel for line identifications).

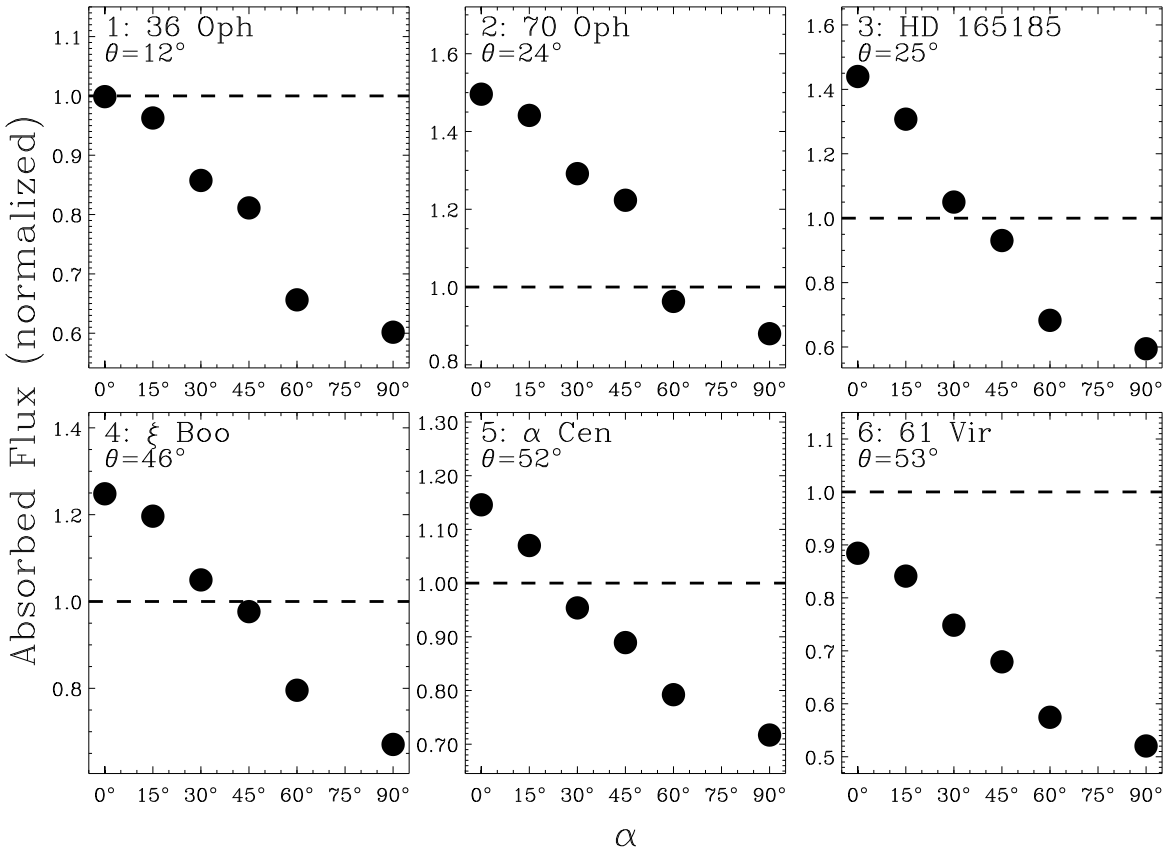

Fig. 5.— For six upwind lines of sight, the predicted wavelength-integrated Lyα flux absorbed by heliospheric H I beyond that absorbed by the ISM is computed for the six models from Fig. 3 and plotted versus α, the ISM field orientation relative to the ISM flow direction. The fluxes are normalized to the observed amount of flux absorbed, so in each panel a flux of 1 (dashed lines) corresponds to agreement with the data.

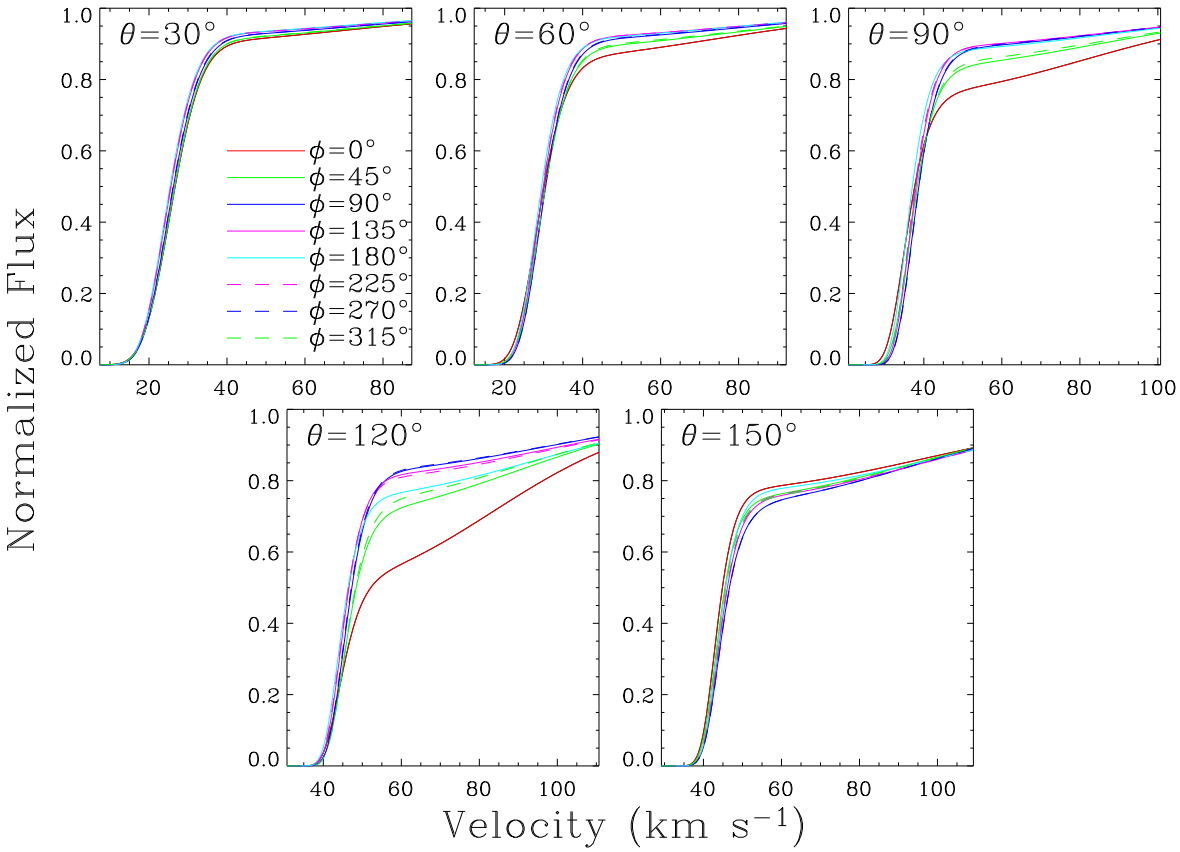

Fig. 6.— An illustration of the directional dependence of H I Lyα absorption predicted by a 3D MHD heliospheric model assuming an ISM field strength and orientation of $B = 2.5$ μG and $\alpha = 45°$, respectively. Absorption is shown for five values of the poloidal angle θ (the angle between the line of sight and the upwind direction of the ISM flow), and eight values of the azimuthal angle ϕ (where the plane of the ISM magnetic field is in the $\phi = 0°$ and $\phi = 180°$ directions). The model grid does not extend far enough downwind to properly search for azimuthal absorption variations at $\theta = 150°$.